Journal of Pharmaceutical Sciences 114 (2025) 449–457

Contents lists available at ScienceDirect

Journal of Pharmaceutical Sciences

journal homepage: www.jpharmsci.org

Pharmaceutics, Drug Delivery and Pharmaceutical Technology

# Counteracting the loss of release for indomethacin-copovidone ASDs

Dominik Borrmann, Pascal Friedrich, Justin Smuda, Gabriele Sadowski*

*Department of Chemical and Biochemical Engineering, Laboratory of Thermodynamics, TU Dortmund University, Figge-Str. 70, D-44227 Dortmund, Germany*

ARTICLE INFO

*Article history:*
Received 9 October 2024
Revised 13 October 2024
Accepted 13 October 2024
Available online 6 November 2024

*Keywords:*
ASDs
Water sorption
API release
Loss of release
Phase diagrams
Diffusion

ABSTRACT

This work revisits the changing release behavior of indomethacin(IND)-copovidone amorphous solid dispersions (ASDs) when increasing their drug load (DL). While showing congruent release behavior at DL 0.1, ASDs with DLs of 0.3 and higher show incongruent release finally resulting in a complete loss of release. To study and explain this phenomenon, we modeled the release kinetics of these ASDs and looked into their phase behavior both experimentally and theoretically. We applied a diffusion model to accurately describe experimental release profiles for congruent release, incongruent release as well as for loss of release. Predicted concentration profiles for IND, copovidone, and water within the ASD revealed the formation of an ASD layer that almost exclusively contains amorphous IND. Our phase-diagram predictions and experimental data explain this phenomenon by water-induced phase separation in those parts of the ASD which did absorb water from the dissolution medium. Whereas the evolving copovidone-rich phase dissolved, the IND-rich phase remained undissolved and formed a super-hydrophobic cover of the remaining inner core of the ASD, thus finally completely preventing its dissolution. Higher DLs promote phase separation. This leads to the counterintuitive effect that the higher the DL, the lower the absolute amount of IND released. While the ASD containing 6 mg IND (DL 0.1) released 6 mg IND, the one containing 42 mg IND (DL 0.7) released only 1 mg IND. The theoretical approach applied in this work is for the first time able to quantitatively predict that reducing DL or tablet size could be used to overcome this problem.


## Introduction

The bioavailability of an active pharmaceutical ingredient (API) with low water solubility can be enhanced by dissolving the API in a polymer matrix generating an amorphous solid dispersion (ASD). Upon dissolution of the water-soluble polymer into an aqueous environment, the API is simultaneously released from the ASD. This phenomenon is known as congruent-release behavior. One could state that the API is "carried along" by the high release rate of the hydrophilic polymer. An earlier study concluded that the API release of most ASDs with an hydrophobic API and a hydrophilic polymer show congruent release for low drug loads (DLs).[1]

Required API doses and size limitations of tablets require ASDs with higher DL. However, a breakdown of API release is sometimes observed when increasing the DL beyond a certain value.[2] The DL at which the breakdown in the release of the API not in the one of the polymer is observed is called limit of congruency (LoC). Saboo et al.[2,3] extensively investigated the LoC phenomenon experimentally. Nilvadipine-copovidone ASDs and cilnidipine-copovidone ASDs showed a breakdown in API release at DLs of 0.15 and 0.2, respectively, while the polymer release only decreased but did not break down.[2] This LoC behavior was explained by suggesting that an insoluble API barrier did form at the surface of the ASD, thus preventing further release of the API. X-ray photoelectron spectroscopy of the ASD surface after release supported this hypothesis. Furthermore, the authors postulated that amorphous-amorphous phase separation (AAPS) within the ASD might be responsible for the API enrichment at the surface. They assumed that the ASD did absorb water and then demixed in polymer-rich domains and API-rich domains, whereas the polymer-rich domains were easily released while the poorly-water soluble API-rich domains remained in the ASD-water interface.

A similar behavior was observed for a copovidone-ritonavir ASD when increasing the DL beyond 0.25.[3] Krummnow et al.[4] were able to explain the LoC and to determine the DL at which it is observed by predicting AAPS in the polymer/API/water system. They could show that the LoC is a direct consequence of AAPS and that the latter can even be predicted the using the Perturbed-Chain Statistical

* Corresponding author.
*E-mail address:* Gabriele.Sadowski@tu-dortmund.de (G. Sadowski).

https://doi.org/10.1016/j.xphs.2024.10.022

Associating Fluid Theory (PC-SAFT)[5] consequently supporting the earlier AAPS hypothesis.[4]

On a further note, Dohrn et al.[6] identified another type of breakdown in API release were dissolution is accompanied by a rapid crystallization of the API at the surface. This was observed in a naproxen-copovidone ASD resulting in a passivation of the ASD by naproxen crystals. As a result, the release of both API broke down at a certain DL (loss of release, LOR). Recently, the groups of Taylor and Sadowski[7] commonly investigated the LoC behaviors with special on AAPS and the resulting morphology of the demixed ASDs[7]. Copovidone-based ASDs of different DLs were stored at RHs close to unity. Hydrophobic and hydrophilic dyes where used to visualize polymer-rich and API-rich domains. A PC-SAFT-predicted phase inversion from API droplets embedded in a continuous polymer phase into polymer-water droplets embedded in an continuous API phase was observed for DLs corresponding to the LoC. As a consequence, it was shown that the phase behavior within the ASD and the release behavior of the ASD are inherently coupled.

Deac et al.[8] showed that the LoC of ASD with phenolphthalein derivates that had stronger associative interactions with copovidone were much lower compared to ASDs with API that only weakly associate with copovidone.

Li et al.[9] reported the negative impact of the water-induced AAPS on the release behavior even during spray drying . Spray-dried ASDs prepared from water-based solutions showed lower API release compared to those prepared from water-free solutions. Moreover, they discussed the importance of the copovidone-API interactions on the LoC. Que et al.[10] reported a positive influence of hydrophilic surfactants on the LoC.

Thus, understanding the API release from ASDs has been greatly advanced by investigating the phase behavior of the wet ASD. However, the quantitative amounts of API or polymer released over time is to a great extent determined by diffusion processes.[11] There exist a lot of empirical but also mechanistic models to quantify API release as summarized by Peppas and Narasimhan.[11] While most models consider API and/or polymer releases into the surrounding aqueous medium, simultaneous consideration of both water sorption and API/polymer releases was not performed yet. The well-known Stefan-Maxwell diffusion model is most suitable to describe such multicomponent diffusion processes.[12] This model in general allows obtaining time-dependent concentration profiles of all species at each position within the ASDs during dissolution.

In this work, we therefore revisited the LoC observed for copovidone-based ASDs investigating IND-copovidone ASDs as an example. We demonstrate that our diffusion model is able to reproduce both congruent and incongruent release profiles of ASDs and to accurately depict the API-enrichment on the ASD surface which is usually observed during the release of copovidone-based ASDs. based on correlating the experimentally-determined release profiles, we predict the DLs and ASD dimensions that ensure complete ASD release.

## Modeling

### *Release kinetics*

A sketch of the ASD during a release experiment is provided in Fig. 1a.

The ASD is placed inside a metallic compartment of the stirrer. Using this setup, only one side of the ASD is exposed to the surrounding water and thus only the spatial dimension z along the thickness L of the ASD is relevant for mass transfer (Figs. 1b and 1c). API and polymer are released into the surrounding water with an API mass flux $\dot{m}_a$ and a polymer mass flux $\dot{m}_p$ and at the same time water enters the ASD. Considering the water flux $\dot{m}_w$ into the ASD is crucial, since copovidone-based ASDs are known to absorb significant amounts of water during storage at humid conditions[13] and a dissolution vessel is the most humid environment imaginable (relative humidity (RH) close to unity).

As the dissolution medium is usually well mixed, we assume that the diffusion of both API and polymer from the ASD interface into water is the rate limiting step and rather than their distribution within the dissolution medium. The diffusive mass fluxes $\dot{m}_i$ of API, polymer, and water were calculated using the an segmental Maxwell-Stefan (MS) approach in Eq. (1) as first proposed by Fornasiero et al.[14]

$$\nabla w_i = \sum_{j \neq i}^{n} \frac{w_j \dot{m}_i - w_i \dot{m}_j}{Đ_{ij}} \tag{1}$$

Here, $n$ is the number of components, $\nabla w_i$ is the weight fraction gradient of component $i$. $\dot{m}_i$ and $w_i$ are the mass flux and the mass fraction of component $i$, respectively. $\rho_i = w_i \rho$ is the mass concentration of component and $\rho$ is the density of the mixture. We considered a one-dimensional diffusion along the spatial dimension $z$, so $\nabla = \frac{\partial}{\partial z}$. Lastly, $Đ_{ij}$ is the apparent MS diffusion coefficient of component $i$ in $j$. Eq. (1) was solved for the mass fluxes as described in Eq.S1-S6 in the Supplementary material.

Quantifying the diffusive mass fluxes $\dot{m}_i$ of API, polymer, and water allowed us to determine the weight fractions $w_i(t,z)$ of these

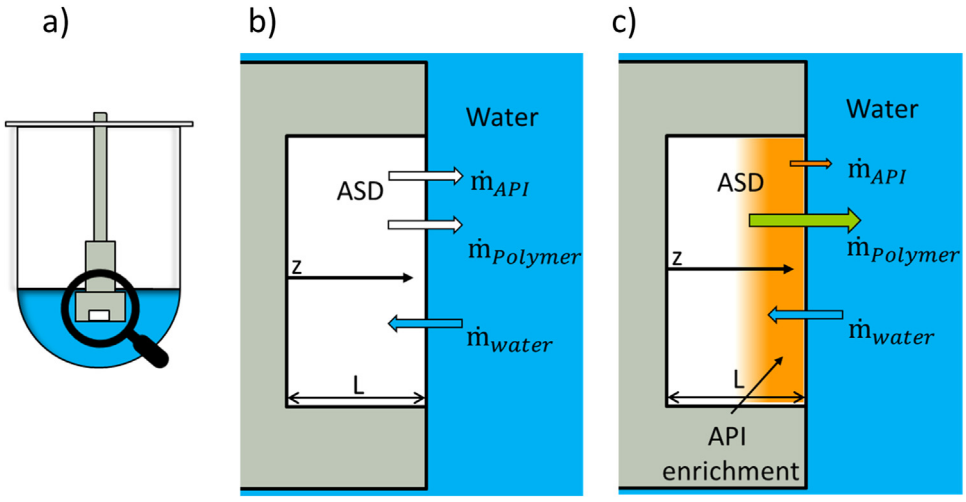


**Fig. 1.** Schematic of an ASD within in a USP-II vessel during a release experiment (a). Zoom into the ASD-water interface for congruent release (b) and incongruent release (c).

components at each point in the wet ASD as function of time. Finally, the $release_i$ of a component i (API or polymer) is defined as the ratio of the released mass $m_i(t)$ of that component, the initial mass $m_{ASD}$ of the ASD and the initial DL. Thus, the releases of API and polymer were calculated according to Eq. (2) and Eq. (3), respectively.

$$release_a(t) = \frac{m_a(t)}{DL\ m_{ASD}} \tag{2}$$

$$release_p(t) = \frac{m_p(t)}{(1-DL)m_{ASD}} \tag{3}$$

Water-sorption kinetics

Eq. (1) simplifies when considering the water sorption of an ASD at humid conditions. Then, only the water flux in to the ASD needs to be considered.

$$\dot{m}_w = \rho_w \frac{D_w}{1-w_w} \nabla w_w \tag{4}$$

Here, $D_w$ is the apparent water diffusion coefficient in the ASD. Eq. (4) is in fact identical to the diffusion model used to predict the water-sorption kinetics in ASDs from our previous study.[13] The water sorption equilibria of the IND-copovidone ASD at 0.95 RH were also predicted as described in that study.[13]

*Amorphous-amorphous phase separation*

Phase-separation calculations were utilized to explain the LoC behavior observed for the investigated ASDs. For that purpose, we considered the equilibrium conditions for two coexisting liquid phases, labeled L1 and L2, according to Eq. (5).

$$x_i^{L1}\gamma_i^{L1} = x_i^{L2}\gamma_i^{L2} \tag{5}$$

Here, $x_i^{L1}$ and $x_i^{L2}$ represent the mole fractions of component (i) in phases L1 and L2, respectively. The activity coefficients $\gamma_i^{L1}$ and $\gamma_i^{L2}$ of component (i) in the two phases L1 and L2 account for the interactions between all molecules and depend on the compositions of the two phases. The activity coefficients were determined in this work using the Perturbed-Chain Statistical Associating Fluid Theory (PC-SAFT) as described in the PC-SAFT section.

*Glass transition temperature*

The glass transition temperature $T_g$ of a wet ASD was predicted using the Gordon-Taylor equation in Eq. (6).

$$T_g = \frac{\sum_i K_i w_i T_{g0i}}{\sum_i K_i w_i} \tag{6}$$

Here, $K_i$ is the Gordon-Taylor parameter of component $i$ and $T_{g0i}$ is the glass transition temperature of the component $i$.

Perturbed-chain statistical associating fluid theory (*PC-SAFT*)

PC-SAFT was used to calculate the activity coefficients $\gamma_i$ of all components $i$ using textbook thermodynamics. PC-SAFT describes the reduced residual Helmholtz energy $a^{res}$ of a mixture according to Eq. (7).

$$a^{res} = a^{hc} + a^{disp} + a^{assoc} \tag{7}$$

$a^{hc}$ is the reduced Helmholtz energy contribution for the hard-chain reference fluid. $a^{disp}$ is the dispersion contribution accounting for van der Waals attractions, and $a^{assoc}$ is the association contribution. The equations for $a^{hc}, a^{disp}, a^{assoc}$ can be found in the literature.[5] The pure-component parameters are the segment diameter $\sigma_i$, the segment number $m_i^{seg}$, the association volume $\kappa^{AiBi}$, the dispersion energy parameter $\frac{u_i}{k_B}$ and the association energy parameter $\frac{\varepsilon^{AiBi}}{k_B}$ of component $i$. The average segment diameter in a mixtures $\sigma_{ij}$, and the dispersion energy between unlike molecules $u_{ij}$ were calculated using Berthelot-Lorenz mixing rules. The cross-association energy $\varepsilon^{AiBj}$ and the cross-association volume $\kappa^{AiBj}$ were calculated using Wolbach and Sandler[15] mixing rules. The reliability of these mixing rule was intensively investigated in previous studies.[16] The dispersion energy of the mixture was corrected based on Eq. (8).

$$u_{ij} = (1-k_{ij})\sqrt{u_i u_j} \tag{8}$$

Here, $k_{ij}$ is the binary interaction parameter between component $i$ and component $j$.

*Model parameters*

PC-SAFT pure-component parameters and the parameters of the Gordon-Taylor equation were taken from earlier works[13] and are summarized in Table 1. The binary interaction parameters $k_{ij}$ for PC-SAFT are summarized in Table 2. The apparent MS Diffusion coefficients $Đ_{ap}$, $Đ_{pw}$, $Đ_{aw}$ were obtained in this study by fitting them to the release profiles of ASDs with a thickness of 1 mm measured as described in section release experiments and are summarized in Table 3. The apparent water diffusion coefficients $D_w$ in the ASD were obtained by fitting to experimental data for water-sorption kinetics in the ASDs at an RH of 0.95 and a temperature of 25 °C. They are also summarized in Table 3. $Đ_{ap}$, $Đ_{pw}$, $Đ_{aw}$ are the apparent diffusion coefficients of the API in the polymer, of the polymer in water and of the API in water, respectively. These diffusion coefficients describe the mobility between polymer, API, and water based on the mass transfer observed in the release experiments. $D_w$ describes the mobility of water in the ASD.

## Materials and methods

*Materials*

Copovidone (poly (vinylpyrrolidone-co-vinyl acetate) 64) (CAS ID: 25086-89-9) with an average molar mass 65 kg/mol and indomethacin (IND) were purchased from Dow Chemicals and from TCI (CAS ID: 53-86-1). Water used for the release and sorption measurements was taken from a Millipore® purification apparatus from Merck.

**Table 1**
PC-SAFT pure-component parameters and parameters of the Gordon-Taylor equation used in this work.

| | $M_i$ g mol$^{-1}$ | $m_i/M_i$ mol g$^{-1}$ | $\sigma_i$ /Å | $u_i/k_B$ /K | $\kappa^{AiBi}$ /- | $N_i$ /- | $\epsilon^{AiBi}/k_B$ /K | $K_i$ /- | $T_{g0i}$ /K |
|---|---|---|---|---|---|---|---|---|---|
| copovidone 65,000 | | 0.0372 | 2.947 | 205.27 | 0.02 | 653/653 | 0 | 0.3 | 383.9 |
| IND | 357.79 | 0.0399 | 3.535 | 262.79 | 0.02 | 3/3 | 886.44 | 0.11 | 317.6 |
| Water | 18.02 | 0.0669 | 2.797 | 353.94 | 0.045 | 1/1 | 2425.67 | 1 | 136 |

Parameters taken from[13].

**Table 2**
PC-SAFT binary interaction parameters $k_{ij}$ used in this work.

| Component i | Component j | $k_{ij}$ /- |
|---|---|---|
| Copovidone | IND | −0.0621 |
| Copovidone | Water | 0.156 |
| Water | IND | −0.025 |

binary interaction parameters taken from.[13]

**Table 3**
Water diffusion coefficients $D_w$ in the ASD at a RH of 0.95 and apparent MS diffusion coefficients $Đ_{ij}$ between components *i* and *j*, all at 25 °C. *a* stands for the API (IND), *p* stands for the polymer (copovidone) and *w* stands for the water.

| | $Đ_{ap}$ $m^2\ s^{-1}\ 10^{-13}$ | $Đ_{aw}$ $m^2\ s^{-1}\ 10^{-13}$ | $Đ_{pw}$ $m^2\ s^{-1}\ 10^{-13}$ | $D_w$ $m^2\ s^{-1}\ 10^{-13}$ |
|---|---|---|---|---|
| DL=0.1 | 442.29 | 3998.48 | 3057.40 | 132.15 |
| DL=0.3 | 2.7 | 7.111 | 8543.12 | 93.19 |
| DL=0.5 | 0.1 | 0.269 | 7.962 | 26.38 |
| DL=0.7 | 0.1 | 0.2375 | 3.589 | 9.22 |

*Vacuum compression molding*

ASD discs of copovidone and IND were prepared by vacuum compression molding. Prior to the compression molding, ASD powder blends of copovidone and IND were prepared using a ball mill (pulverisette 23 from Fritsch). Following that, these ASD powder blends were placed on a glass slide (⌀ 8 mm) within the cylindrical mold (⌀ 8 mm) of the vacuum-compression molding tool from MeltPrep GmbH (Graz, Austria). Then, the mold was closed and vacuum was applied. After that, the mold was heated up to 140 °C for the ASD with a DL 0.1, to 110 °C for the ASD with a DL 0.3, to 117 °C for the ASD with a DL 0.5, and to 155 °C for the ASD with a DL 0.7. These temperatures were held 15 min for the ASDs with DLs of 0.1 and 0.3, 10 min for the ASD with a DL 0.5, and 1 min for the ASD with a DL 0.7. Finally, the cylindrical mold was cooled for 15 min using pressured air and the ASD disc was removed from the mold. After preparation, a fine balance (Mettler Toledo) with 0.1 mg precision was used to determine the mass of the ASD disc. We aimed to prepare ASD discs for each DL with 1 mm thickness which weighed on average 62.53± 1.6 mg and ASD discs of 0.25 mm thickness which weighed on average 15.27±0.9 mg. The thicknesses of the ASD discs were estimated by dividing their mass by the density of the ASD and the lateral area of the cylindrical ASD. The density of the ASD varied with DL and was estimated by neglecting excess volume and knowing the density of copovidone (1190 kg/ $m^3$) and amorphous IND (1320 kg/$m^3$). On average, the thicknesses of the ASDs with DLs of 0.1 were 0.995 mm and 0.247 mm, of ASDs with DLs of 0.3 were 1.007 mm and 0.2519 mm, of ASDs with DLs of 0.5 were 1.006 mm and 0.2516 mm, and of ASDs with DLs 0.7 were 1.005 mm and 0.249 mm.

*Water-sorption measurements*

The dynamic vapor sorption (DVS) apparatus (Intrinsic Plus from Surface Measurement Systems) was used to measure the water sorption of the ASDs with a precision of 0.1 $\mu$g. We used the same DVS device as in our previous studies.[13] We used nitrogen as the inert gas with a total volume flow of 200 ccm. The temperature was kept constant at 25 °C. The prepared ASD discs were dried at least 300 min to gain their dry mass. Then, the RH was changed from RH = 0 to 0.95, whereas RH was kept constant for 300 min. The mass of water was obtained as the difference between the total mass reading and the dry mass of the ASD.

*Release experiments*

The release behavior of ASDs with different DLs was investigated in a USP-II apparatus from SOTAX (AT 7Smart). 500 g of ultrapure water (Millipore) was weighted into the vessel. Then, an ASD disc, manufactured as described in the section *vacuum compression molding,* was stuck to the stirrer blade immediately after preparation. We stuck the ASD tables in the stirrer blade to create only one interface between the ASD and the aqueous dissolution medium. The stirrer speed was set to 250 rpm and the water bath was preconditioned to 25 °C. The stirring speed was set rather high to ensure that the medium is well mixed. Moreover, this very high stirring speed avoids release limitations imposed by a poor distribution of API and polymer in the dissolution medium and thus allows to specifically study the water/polymer/API diffusion within the ASD as this becomes the rate-limiting step for release. Samples (1 mL per sample) were withdrawn from the dissolution medium at different time instances and analyzed using UV–VIS spectroscopy (Specord 210 plus from Analytik Jena). As in other studies,[17,18] the samples were not filtered prior to UV–VIS Analysis. Thus, we did no differentiate between the API/polymer masses truly dissolved compared to those released as nanodroplets. Thus, the measured release describes the masses of polymer and API which left the ASD. Calibration curves at wavelengths of 220 nm and 240 nm were recorded beforehand and can be found in Figure S1 of the supplementary materials. These wavelengths correspond to the shoulder regions of the peaks from copovidone and IND, respectively. Measuring at both wavelengths allowed to differentiate the two components in solution. All release experiments were performed as triplicates and average values are reported with the standard deviation as error bars .

*Microscopy*

An optical microscope (Leica DM4000 M) was used for image acquisition of the inner of the ASD discs after 300 min of release experiment. The ASD discs were cut, turned to the side and viewed under the microscope at 5x magnification.

*Powder X-ray diffraction (PXRD) measurements*

After the release experiment, PXRD measurements of the white ASD layers (see Fig. 4c) were performed using a PXRDMini Flex 600 device from Rigaru. A Cu-K-$\alpha$ irradiation source (voltage of 40 kV and a current of 15 mA) was used to investigate the angular velocity $\theta$ in range of $5° < 2\theta < 30°$ with a step size of 5° $min^{-1}$ in a spatially-fixed Brag-Brentano geometry.

*Dynamic scanning calorimeter (DSC) measurements*

The ASD discs, their cores and their layers were measured via DSC (Q2000 from TA Instruments, Eschborn, Germany) before and after release the measurements. The ASDs or their scrapped-off layers were weighted into an aluminum pan (THEPRO, Heinsberg, Germany). A hole was punched into the pan lid and the sample was dried in the DSC at 25 °C for 300 min using pure nitrogen (50 mL $min^{-1}$). The DSC was utilized to modulate the temperature in a range from 0 °C to 190 °C with a heating rate of 5 K $min^{-1}$.

*Erosion tests*

Using ASD films, images of the ASDs when in contact with liquid water were created. About 15 mg of the same ASD powder used for the ASD discs was weighted on a circular coverslip (⌀18 mm) and placed onto a hotplate at 160 °C for 2 min. Then another coverslip was used to sandwich the ASD melt between the two coverslips.

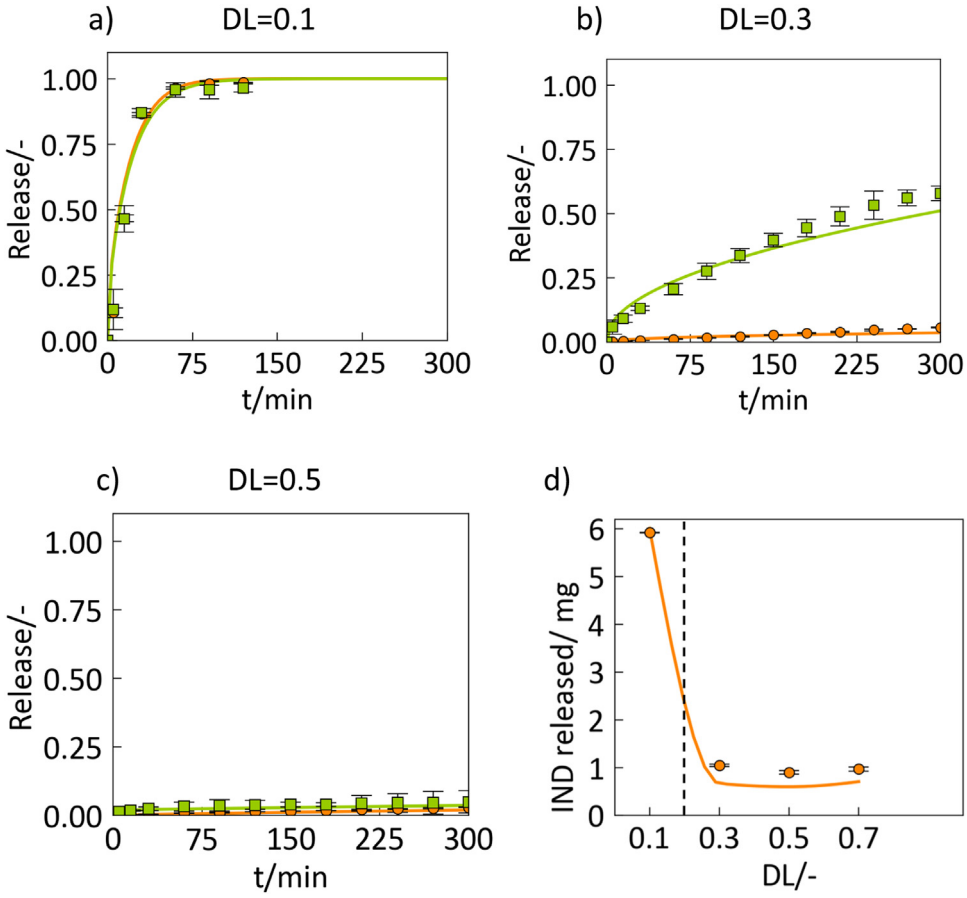


**Fig. 2.** Releases of IND and copovidone from IND-copovidone ASDs of 1 mm thickness and with initial DLs of 0.1 (a), 0.3 (b), and 0.5 (c) at 25 °C. Experimental data points are displayed as squares for copovidone and as circles for IND. Calculations using the diffusion model (Eq. (1)) are displayed as solid lines. (d) released mass of IND after 300 min as a function of the ASD DL. Circles are experimental data and the line is the description using the diffusion model (Eq. (1)). The LoC of DL 0.2 determined from literature[19] is indicated as dashed line.

Finally, the ASD-coverslip sandwich was removed from the hotplate and placed on a petri dish, which was filled with ~20 ml of ultrapure water at 25 °C. Images were taken after 90 min.

## Results and discussion

### *Release kinetics*

Fig. 2a-c show the measured and modeled release kinetics of ASDs with DLs of 0.1, 0.3, and 0.5 in water. The release of IND was found to be highest for the ASD with the lowest DL 0.1 (Fig. 2a). After 70 min, the complete masses of both IND and copovidone were released from the ASD. Here, congruent release was observed. For the ASD with a DL 0.3 (Fig. 2b), the release behavior became incongruent as the IND release was only 5 % after 300 min while the copovidone release was still 58 %. Earlier reports[19] observed the LoC of IND-copovidone ASDs at a DL 0.2 and thus agree with our release experiments. For the ASD with a DL 0.5 (Fig. 2c), the copovidone release finally also broke down to the same level as the IND release (LOR) .[19]

The poor release behavior of ASDs with DLs higher than the LoC (about 0.2[19]) opposed to the ones with lower DLs can even better be seen in Fig. 2d. Despite the fact that the absolute mass of IND increased from 6 mg for the ASD with a DL 0.1 to almost 42 mg for the ASD with a DL 0.7, only 1 mg of IND was released into the dissolution medium for all ASDs having DLs 0f 0.3 and higher.

Counterintuitively, the higher the drug load of the ASD, the lower the absolute mass if IND released. Thus, increasing the DL beyond the LoC does not increase the mass of released IND, but only increases the mass of IND remaining undissolved in the ASD.

### *Water-sorption kinetics*

The water-sorption kinetics in IND-copovidone ASDs of different DLs measured at RH =0.95 and 25 °C are displayed in Fig. 3. The water-diffusion coefficients $D_w$ (Table 3) were fitted to the water sorption kinetics of the ASDs with 1 mm thickness (Fig. 3a) and are shown as function of DL in Fig. 3b.

Due to the hydrophobicity of IND, the ASDs with the lowest DL 0.1 absorbed the most water compared to the ASDs with higher DLs. The water diffusion coefficient drastically decreases with increasing DL which means that ASDs with higher DLs absorb water not only to a lower extend but also much slower than ASDs with lower DLs. However, the most drastic decrease in the water diffusion coefficient is observed when DL exceeds values of 0.3.

Layer formation and IND enrichment

Fig. 4a displays the ASD before the release experiment. The yellowish ASD disc was amorphous and transparent. Fig. 4b shows the same ASD after the release experiment. It can be seen that a white, non-transparent layer formed during the exposure to water.

The water penetration can be evaluated using the well-known Einstein-Smoluchowski relation[20] by estimating the water-penetration depth in the ASD in Table 4 using the water diffusion coefficients $D_w$ determined from the water sorption kinetics. The water-penetration depth was calculated according to $\sqrt{2D_w t}$ . It is compared to

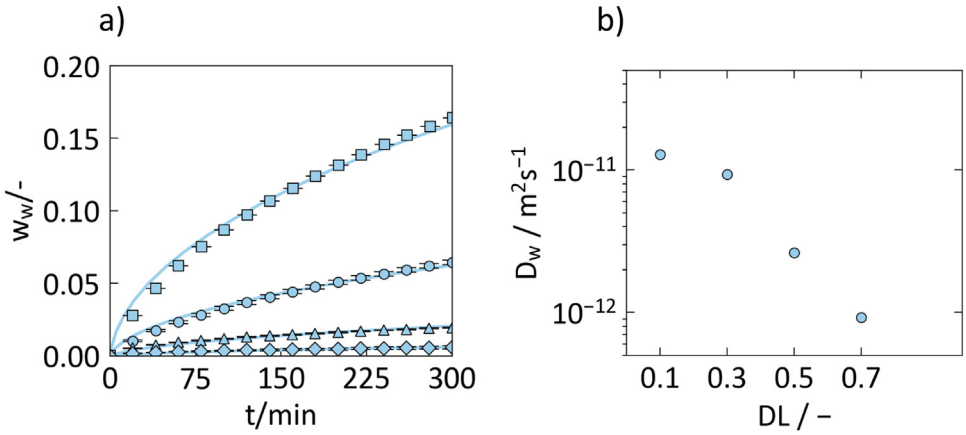


**Fig. 3.** (a) Water weight fraction $w_w$ absorbed in IND-copovidone ASDs with a thickness of 1 mm at 25 °C and 0.95 RH. DL= 0.1 (squares), initial DL= 0.3 (circles), DL= 0.5 (triangles) and DL=0.7 (diamonds). Regressions by the diffusion model (Eq. (4)) are displayed as solid lines. (b) Water diffusion coefficient $D_w$ in the ASD as a function of ASD drug load.

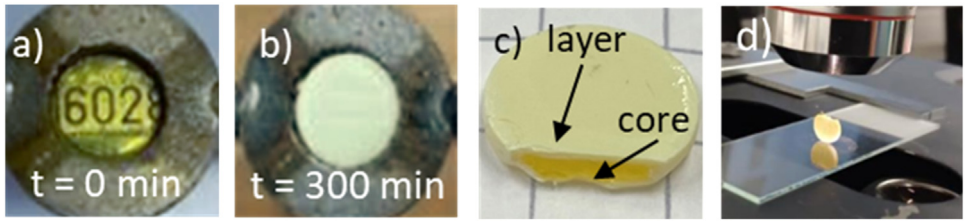


**Fig. 4.** An ASD disc with an initial DL 0.5 stuck on a stirrer blade before the release experiment (a) and after the release experiment (b). The ASD was removed from the stirrer blade and cut so that its inner core became visible (c). The ASD was turned on its side and viewed under the microscope (d).

microscopic images of the ASDs taken after the release experiments presented in Fig. 5 where the thickness of the layer was estimated using the scale of the image.

Fig. 5 reveals microscopy images of the ASDs with initial DLs of 0.3 and 0.5 after 300 min of release experiment. In both cases, a layer formed around the ASD disc (Fig. 4c). For the ASD with an initial DL 0.3 (Fig. 5a), the experimentally determined layer accounted for ~64 % of the disc volume, whereas it was only ~23 % of the disc for the ASD with an initial DL 0.5 (Fig. 5b). The predicted water penetration depths of ~57.9 % for DL 0.3 and ~30.8 % for DL 0.5 (Table 4) agree quite well with the measured extent of these layers.

ASD cores and layers were separated using a razor blade and measured individually in the DSC as described in section *DSC measurements*. The glass-transition temperatures of the cores agree very well with the glass-transition temperatures of the dry ASDs before the release experiment (Fig. 5). Thus, the cores of the ASDs remained unchanged during the release experiments. Furthermore, no melting peaks the layers were observed by neither DSC nor PXRD measurements. Thus, no IND crystallization happed there during the release experiment. Additionally, the outer parts of the layers were dissolved separately in water and the solution was analyzed using the same UV −VIS spectroscopy method as described in the section *release experiments*. This analysis revealed that this layer mostly consisted of amorphous IND and water (see Supplementary Material). Apparently, most copovidone dissolved from the ASD layer leaving the IND layer behind. Fig. 5a and 5b also show the predicted axial course of water weight fraction and IND concentration (DL) in the ASDs after 300 min (as described in the section Release kinetics). The transitions between core and layer (below and above 10 wt% water) in Fig. 5 coincide with the regions of low and high water contents (right axes). Thus, the presence of water is a prerequisite for the layers formation (see also section *Ternary phase diagram*) and the depth of the water penetration is thus a suitable measure for the layer depth (Table 4).

Moreover, the DLs in the core (starting at $z$ = 0 mm) correspond to the initial DLs of 0.3 and 0.5. Moving to the right (outwards), the predicted local DLs after 300 min rapidly increase towards almost being one (almost pure IND) directly at the interface between the ASD and the dissolution medium ($z$ = 1 mm). This means, we predicted the formation of a layer consisting of amorphous IND only, which perfectly fits the phenomena experimentally observed in similar studies,

**Table 4**
Comparison of measured layer thickness (Fig. 5) and calculated water-penetration depth for 1 mm IND-copovidone ASDs at 25 °C after 300 min of release experiment. Layer thickness and water penetration depths are given as percentages from the original thickness of the ASD.

| | DL=0.3 | DL=0.5 | DL=0.7 |
|---|---|---|---|
| Layer thickness | 63.8 % | 23.2 % | 12.1 % |
| Water-penetration depth | 57.9 % | 30.8 % | 18.21 % |

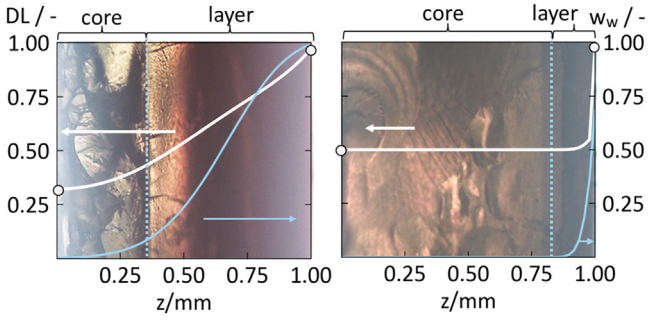


**Fig. 5.** Microscope images of the ASDs after the release experiments after 300 min at 25 °C and modeled drug-load profiles (white lines, left axes) and water weight fractions in the ASD (light blue lines, right axes) predicted by the diffusion model (Eq. (1)). Initial DL=0.3 (left) and an initial DL=0.5 (right). Measured drug loads in the core ($z$ = 0) and the outer part of the layer ($z$ = $L$ = 1 mm) are displayed as circles. Vertical dotted lines indicate the transition between core and layer of the ASDs.

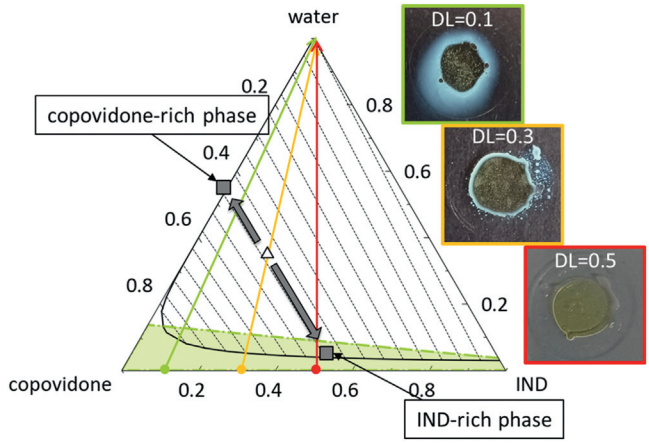


**Fig. 6.** Phase diagram of the IND-copovidone-water system at 25 °C. The solid black line frames the region of AAPS and was calculated using Eq. (5)). The green dashed-dotted line indicates the glass transition of the ASD predicted by the Gordon Taylor equation (Eq. (6)). In the green area below this line, the ASD is glassy. Arrows show the pathways for ASDs of different initial DLs (DL 0.1 green, DL 0.3 yellow, DL 0.5 red) during the release experiment. The white triangle exemplifies the demixing of a wet ASD with a DL 0.3 in the AAPS region along a tie line (dashed black lines). Images form the erosion tests of ASD films with DLs 0.1; 0.3; and 0.5 in liquid water are shown on the right.

which investigated the release behavior of copovidone-based ASDs (e.g. Saboo et al.[2] and Indulkar et al.[3]).

After 300 min, the layer is much larger for the more hydrophilic ASD with DL 0.3 (Fig. 5a) than in the more hydrophobic ASD with DL 0.5 (Fig. 5b) as the former absorbs much more water than the latter. The presence of water increases the mobility in the layer allowing fast release of the polymer. However, the API is much less water-soluble than the polymer and thus the API enriches in the layer which leads to the observed loss of API release in both cases. As long as the layer is large (as for DL 0.3), polymer continues to release. In case of a small layer (ASD with DL 0.5), the amount of releasable polymer is low and polymer diffusion from the core into the layer takes quite long. As a result, the polymer release of this ASD collapses quite fast leading to the LOR or the ASD with DL 0.5.

*Ternary phase diagram of the wet ASD*

The phase diagram of the IND-copovidone-water ternary system predicted by PC-SAFT is displayed in Fig. 6. As it can be seen, PC-SAFT predicts a large AAPS region caused by the immiscibility of the IND and water. ASDs with compositions within this AAPS region (for example due to water sorption) will separate into a polymer-rich phase and an API-rich phase.

The release of the ASD in water can be considered as mixing a dry ASD with water in the phase diagram, this can be visualized by connecting both states by a straight line. As example, for an ASD with a DL 0.1, we move along a line that connects this point on the lower side of the triangle with the upper edge of the triangle which indicates pure water. As shown in various previous works,[4,6,7] AAPS may occur in ASDs once significant amounts of water were absorbed or in water after significant amounts of the ASD released. This leads to the formation of IND-rich and polymer-rich domains. Evidently, we did observe a large cloudy region in the water surrounding the ASD with DL 0.1 during the erosion test (Fig. 6, right). This cloudy region is a proof for the existence of the AAPS region predicted by PC-SAFT. The release kinetics of the ASD with DL 0.1 is rapid (Fig. 2a) as the small droplets of the IND-rich phase are dragged along the polymer-rich phase.[21,22]

The ASD with DL 0.3 demixes upon water sorption into a continuous IND-rich phase and polymer-rich droplets. This continuous IND-rich phase was quite visible as pronounced bright layer of the ASD (Fig. 6 right, yellow box). IND accumulates near the ASD-water interface and coats the rest of the ASD with a poorly-water-soluble IND barrier. Since the release of the IND-rich phase is poor, IND release quickly breaks down as seen in Fig. 2b. Increasing the DL the ASD beyond this point will not lead to a further increase in IND release since dissolving this IND barrier becomes the rate-limiting step.

The higher the amount of the API-rich phase (i.e. the higher the DL), the sooner this poorly-water-soluble IND barrier builds up. After that happened, neither water is absorbed nor is anything released from the ASD. Therefore, only a small layer is observed for the ASD with DL 0.5 and the releases of both IND and copovidone break down (Fig. 6 right, red box).

*Influence of ASD size*

The diffusion model was finally used to illustrate the effect of ASD size on the release behavior. For this purpose, the IND releases from ASDs with different thickness were predicted using the diffusion model and the diffusion coefficients from Table 3. Whereas all data reported so far were obtained for 1 mm thick ASD films, additional release experiments were performed for ASDs with a thicknesses of 0.25 mm. The predicted and measured masses of IND released into water after 300 min are displayed for different DLs as a function of the ASD thickness in Fig. 7a. Fig. 7b shows the mass of IND not released, i.e., still remaining in the ASDs after 300 min. The predictions of released IND mass from ASDs with a thickness of 0.25 mm

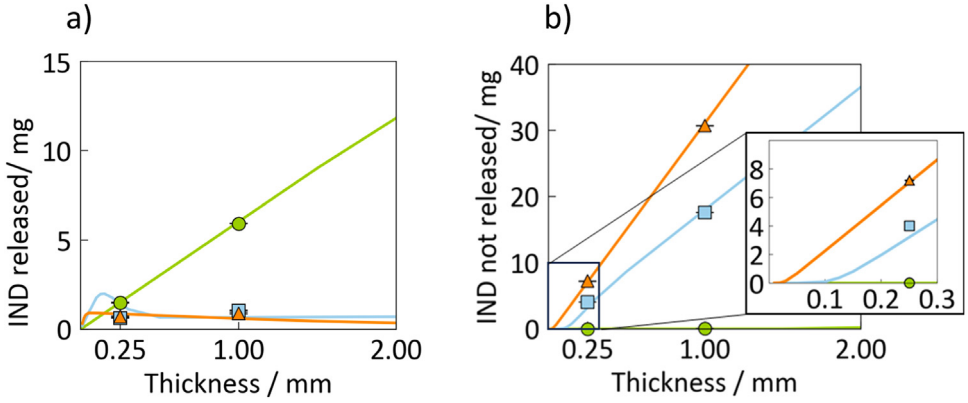


**Fig. 7.** Mass of IND (a) released and (b) not released after 300 min for ASDs with DLs of 0.1 (circles), 0.3 (squares) and 0.5 (triangles). Diffusion-model predictions (Eq. (1)) are displayed as solid lines. The inlet in (b) is a zoom for small film thicknesses.

very well agree the experimental data for all DLs. This validates the release predictions for different thicknesses (sizes) of ASD. For a DL 0.1, the released mass of IND almost linearly increases with increasing ASD thickness (Fig. 7a). This is because, the ASDs with DL 0.1 do not form an outer layer and thus fully dissolve within 300 min even when doubling the film thickness (Fig. 7b). In contrast, ASDs with DLs of 0.3 and 0.5 form a hydrophobic IND layer and therefore the released IND mass remained below 1 mg for a film thickness of 1 mm (see Fig. 5). The thickness of this layer does not depend on the thickness/size of the ASD. Thus, increasing the ASD thickness will only increase the size of its dry core. As a result, the mass of the IND which is not released and remains in the ASD increases drastically with the size of the ASD.

Thus, there are two possibilities to fully dissolve IND from copovidone-based ASDs. The first possibility is to use ASDs with low DLs such as 0.1 (Fig. 2a). These ASDs fully dissolve thus releasing their total amount of IND. If higher DLs are preferred, the size of the ASDs should be reduced far below the thickness of the layer sizes that were observed in Fig. 7. At film thicknesses below 0.1 mm, also the ASD with a DL 0.3 would fully dissolve and no IND would remain in the ASD (inlet of Fig. 7b). As a consequence, the mass of IND released from the ASD of 0.1 mm size and a DL 0.3 shows a maximum where it even exceeds the one of the ASD with a DL 0.1 (Fig. 7a).

## Conclusion

This work revisited the loss of release of both indomethacin (IND) and copovidone from copovidone-based amorphous solid dispersions (ASDs). For that purpose, the release profiles of IND-copovidone ASDs with drug loads (DLs) 0.1, 0.3, 0.5, and 0.7 were investigated. ASDs with a DL 0.1 showed congruent release behavior while ASDs with DL 0.3 and higher showed a breakdown in IND release. This incongruent release behavior was accompanied by a pronounced layer formation at the ASD-water interface. At even higher DLs of 0.5 and 0.7, finally also the polymer release broke down leading to a complete loss of the release for these ASDs. This is consistent with previous reports in the literature that the relative release of IND decreases with increasing amounts of IND in the ASD. However, it's even worse: the more IND an ASD contained, the less was released. Modeling the experimentally determined release profiles allowed predicting the concentrations of all components, i.e. IND, copovidone, and water, at each position in the ASDs at any time during dissolution. The composition profiles revealed the formation of an outer ASD layer containing only IND and water but no copovidone. This was also experimentally verified. These results support established hypotheses from the literature and the role of water-induced amorphous-amorphous phase separation (AAPS) for explaining the incongruent release behavior of ASDs. The thicknesses of the predicted ASD layers, which enclose with an API content identical to one of the initial ASD, agreed very well with the microscopic images.

Ultimately, the reason for the IND enrichment was traced back to an AAPS predicted by PC-SAFT. During their release, the investigated ASDs absorbed water which caused the ASD to demix into IND-rich domains and copovidone-rich domains. While the copovidone-rich domains dissolve, the IND-rich domains form the poorly-water-soluble IND layer, which acts as a coating to the inner of the ASD

Modeling the phase behavior and release kinetics revealed two options to fully dissolve IND-copovidone ASDs. One option is to use ASDs with DLs below 0.3. For those, no layer formation was observed. If higher DLs are required, full release of IND from the ASDs can only be guaranteed if the size of the ASDs is reduced below the size of the layer, here below 80 $\mu$m for the ASD with a DL 0.3 and below 10 $\mu$m for the ASD with a DL 0.5. For that purpose, minitablets with suitable disintegrates would allow for a better partitioning of such particles. Otherwise, significant amounts of polymer and API remain in the ASD and thus will not be released.

This study was conducted for the medium-soluble IND as model API. Most APIs formulated in ASDs are even less soluble in water. This means, that the decrease in API release from these ASDs could be even greater when a API-rich layer forms, as in these cases, the release behavior of the pure API becomes the rate-limiting step.

## Funding

This research received no external funding.

## Declaration of competing interest

The authors declare that they have no known competing financial interests or personal relationships that could have appeared to influence the work reported in this paper.

## Acknowledgements

The PC-SAFT calculations shown in this work were carried out using the software Solcalc. The Solcalc license was provided by amofor GmbH, Dortmund, Germany.

## Supplementary materials

Supplementary material associated with this article can be found in the online version at doi:10.1016/j.xphs.2024.10.022.

## References

1. Craig DQM. The mechanisms of drug release from solid dispersions in water-soluble polymers. *Int J Pharm*. 2002;231(2):131–144.
2. Saboo S, Mugheirbi NA, Zemlyanov DY, Kestur US, Taylor LS. Congruent release of drug and polymer: a "sweet spot" in the dissolution of amorphous solid dispersions. *J Control Release*. 2019;298:68–82.
3. Indulkar AS, Lou X, Zhang GGZ, Taylor LS. Insights into the dissolution mechanism of ritonavir-copovidone amorphous solid dispersions: importance of congruent release for enhanced performance. *Mol Pharm*. 2019;16(3):1327–1339.
4. Krummnow A, Danzer A, Voges K, et al. Explaining the release mechanism of ritonavir/PVPVA amorphous solid dispersions. *Pharmaceutics*. 2022;14(9).
5. Gross J, Sadowski G. Perturbed-chain SAFT: an equation of state based on a perturbation theory for chain molecules. *Ind Eng Chem Res*. 2001;40(4):1244–1260.
6. Dohrn S, Kyeremateng SO, Bochmann E, et al. Thermodynamic modeling of the amorphous solid dispersion-water interfacial layer and its impact on the release mechanism. *Pharmaceutics*. 2023:(5):15.
7. Deac A, Luebbert C, Qi Q, et al. Dissolution mechanisms of amorphous solid dispersions: application of ternary phase diagrams to explain release behavior. *Mol Pharm*. 2024.
8. Deac A, Qi Q, Indulkar AS, et al. Dissolution mechanisms of amorphous solid dispersions: role of drug load and molecular interactions. *Mol Pharm*. 2023;20(1):722–737.
9. Taylor LS, Li N, Cape JL, et al. Water-induced phase separation of spray-dried amorphous solid dispersions. *Mol Pharm*. 2020;17(10):4004–4017.
10. Que C, Lou X, Zemlyanov DY, et al. Insights into the dissolution behavior of ledipasvir-copovidone amorphous solid dispersions: role of drug loading and intermolecular interactions. *Mol Pharm*. 2019;16(12):5054–5067.
11. Peppas NA, Narasimhan B. Mathematical models in drug delivery: how modeling has shaped the way we design new drug delivery systems. *J Control Release*. 2014;190:75–81.
12. Krishna R, Wesselingh JA. The Maxwell-Stefan approach to mass transfer. *Chem Eng Sci*. 1997;52(6):861–911.
13. Borrmann D, Danzer A, Sadowski G. Predicting the water sorption in ASDs. *Pharmaceutics*. 2022;14(6):1181.
14. Fornasiero F, Prausnitz JM, Radke CJ. Multicomponent diffusion in highly asymmetric systems. an extended maxwell-stefan model for starkly different-sized, segment-accessible chain molecules. *Macromolecules*. 2005;38(4):1364–1370.
15. Wolbach JP, Sandler SI. Using molecular orbital calculations to describe the phase behavior of hydrogen-bonding fluids. *Ind Eng Chem Res*. 1997;36(10):4041–4051.
16. Coutsikos, P.; Kalospiros, N.S.; Tassios, D.P. *Capabilities and limitations of the Wong-Sandler mixing rules*; 1995.
17. Indulkar AS, Lou X, Zhang GGZ, Taylor LS. Role of surfactants on release performance of amorphous solid dispersions of ritonavir and copovidone. *Pharm Res*. 2022;39(2):381–397.

18. Siriwannakij N, Heimbach T, Serajuddin ATM. Aqueous dissolution and dispersion behavior of polyvinylpyrrolidone vinyl acetate-based amorphous solid dispersion of ritonavir prepared by hot-melt extrusion with and without added surfactants. *J Pharm Sci*. 2021;110(4):1480–1494.
19. Bochmann ES, Steidel A, Rosenblatt KM, Gessner D, Liepold B. Assessment of the amorphous solid dispersion erosion behavior following a novel small-scale predictive approach. *Eur J Pharmaceut Sci*. 2021:158.
20. Islam MA. Einstein–Smoluchowski diffusion equation: a discussion. *Phys Scr*. 2004;70(2–3):120–125.
21. Han YR, Ma Y, Lee PI. Impact of phase separation morphology on release mechanism of amorphous solid dispersions. *Eur J Pharmaceut Sci*. 2019;136: 104955. (June).
22. Deac A, Qi Q, Indulkar AS, et al. Dissolution mechanisms of amorphous solid dispersions: role of drug load and molecular interactions. *Mol Pharm*. 2023;20 (1):722–737.